ingegneria sismica
International Journal of Earthquake Engineering
Anno XLIII - Num. 1 - 2026

# A Critical-Excitation Response Spectrum Framework for Beyond-Design-Basis Screening of Base-Isolated Nuclear Reactor Buildings

*Naser Khaji*[1] *and Ali Ahmadi*[1,*]

[1] Civil and Environmental Engineering Program, Graduate School of Advanced Science and Engineering, Hiroshima University, 1-4-1, Kagamiyama, Higashi-Hiroshima, Hiroshima 739-8527, Japan

**SUMMARY:** *This paper studies resonance-sensitive seismic demand in a base-isolated nuclear reactor building. The baseline target spectrum is the design response spectrum (DRS) defined in ASCE/SEI 43-19 for seismic design category 5 (SDC 5), which corresponds to a target performance goal of $1\times10^{-5}$ mean annual frequency of exceedance. Beyond-design-basis earthquake (BDBE) levels are represented by controlled multipliers of the same DRS shape (150%, 167%, and 200%). In parallel, a critical excitation (CE) procedure is used to derive a CE-based response spectrum (CE-RS) by maximizing a selected response measure within an admissible input set constrained by physical intensity measures, including peak ground acceleration (PGA), peak ground velocity (PGV), and Arias intensity. The CE constraints are anchored using a recorded event. Response-history analyses are performed using 11 spectrum-compatible horizontal record sets. The reported outputs are peak isolation displacement, isolation-plane base shear, and peak absolute acceleration at the lumped superstructure mass as a global indicator. Results show that BDBE scaling increases demands relative to the DRS baseline, as expected. However, CE-RS produces the largest demands across all metrics, indicating that standard DRS/BDBE scaling may not fully capture resonance-driven isolation demands for long-period isolated systems. A validation check shows that CE results agree closely with CE-RS-based results (differences below about 1%). The proposed workflow provides a fast, traceable supplement for early-stage design screening and for evaluating strengthening or rehabilitation options in existing isolated systems.*

***KEYWORDS:*** *Nuclear power plants; Critical excitation method (CEM); Design-level limit; Response spectrum; Synthetic accelerograms; Beyond-design-basis earthquake (BDBE)*

# 1 Introduction

Nuclear power plants are highly safety-critical facilities, so seismic design is a structural and public-safety requirement. If seismic demands are underestimated, or if key assumptions are unrealistic, damage can reduce safety-related functions. It can also cause long and costly outages. In the worst case, it may affect containment and emergency response systems. The consequences can extend beyond the plant site. They include economic disruption, environmental impacts, and loss of public trust. For this reason, nuclear seismic design and assessment should treat uncertainty carefully and target robust performance under rare, severe shaking [1-3].

*d246266@hiroshima-u.ac.jp
https://doi.org/10.65102/is2026002
Published: 5 April, 2026

Earthquake loading is uncertain because each event is unique and cannot be repeated [4]. Data are also scarce at very strong shaking levels, so our record sets do not fully cover the range of possible source and path effects. Even with careful hazard modelling, large epistemic uncertainty remains, and different models can give noticeably different results, especially at long periods and very low annual probabilities. In addition, real earthquakes may include features that are hard to capture with standard scenarios, such as multi-segment ruptures, basin effects, and time-varying frequency content. For design, this means the next damaging motion may differ from what the available data and typical assumptions suggest, so the evaluation should account for that gap explicitly [4].

Major earthquakes can reveal weak points that were not covered by existing rules. This often leads to code updates. The 1994 Northridge earthquake is a well-known example. It revealed brittle fractures in many welded steel moment-frame connections. After that, design guidance and detailing practice were revised [5]. Similar lessons followed the 1995 Hyogo-ken Nanbu (Kobe) earthquake. Damage observations led to updates in detailing and design rules for several systems. For example, Japan's highway bridge specifications were revised after the event [6]. A common lesson is that the ground motion can include features that control the response, which simple assumptions may not capture well. These include forward-directivity effects and strong velocity pulses [7]. This is why it is reasonable to complement typical scenario thinking with checks that remain safe under adverse, but physically plausible, ground motions.

Recent earthquakes have shown that demand can be controlled by uncommon combinations of duration and spectral content, and sometimes by sequences rather than a single event. The 2010 Maule earthquake (Mw 8.8), for example, produced sustained shaking, and engineering back-analyses used site-specific motions to explain observed deficiencies and structural demands [8]. The 2010–2011 Canterbury earthquake sequence also showed the effect of repeated shaking. Strong events continued for months. Damage levels changed after each event. Safety assessments were updated as the sequence continued [9]. These observations support using hazard-consistent targets when selecting or generating input motions. The targets should also match the key factors controlling the response, not only the spectrum. This includes a duration target when long-duration sources contribute strongly to the hazard. If we use only typical-duration records, collapse risk can be underestimated [10]. When aftershocks are included explicitly, fragility and loss estimates can increase, which reinforces the need to treat sequence effects as part of performance checks when they matter [11].

The 2011 Great East Japan (Tohoku) earthquake is another clear reminder that long-duration shaking with strong long-period content can control demand in flexible and displacement-sensitive systems. Recorded responses and post-event analyses showed that even sites far from the source experienced prolonged motion, which can sustain resonance and accumulate response in lightly damped structures [12]. Detailed studies also emphasized that long-period ground motions during this event carried substantial uncertainty in predominant frequency, duration, and amplitude, which makes typical assumptions risky for performance checks that depend on displacement and drift [13]. Records from instrumented base-isolated buildings show that effective system properties can change during strong shaking. The effective period can shift with response level. Floor accelerations can still be high when higher-mode response is activated. This can happen when dominant motion components align with superstructure modes, even if the isolation layer remains functional [14].

For nuclear installations, seismic design is not treated as a normal code check. The consequences of failure are severe, and the accepted risk is much lower than in conventional

structures. For that reason, major guidance documents expect explicit safety margin beyond the design basis and a clear demonstration that key safety functions are maintained even under rare, high-impact shaking [1-3]. This margin beyond the design basis is often discussed through evaluation of beyond design basis earthquake (BDBE) conditions, i.e., shaking that exceeds the design-basis earthquake used for standard checks. International Atomic Energy Agency (IAEA) guidance, for example, provides recommendations for seismic design and qualification of safety-related Structures, Systems, and Components (SSCs) and also lays out evaluation approaches such as seismic margin assessment and seismic probabilistic safety assessment [1,2]. In U.S. practice, risk-informed performance goals and design criteria are provided in American Society of Civil Engineers (ASCE) standards (with seismic analysis typically handled through ASCE/SEI 4-16 [15] and design criteria through ASCE/SEI 43-19 [3]). This framework also includes checks under BDBE to avoid cliff-edge behavior and to make margin explicit [2]. Risk-informed decision-making is further supported by probabilistic risk assessment (PRA) standards such as American Society of Mechanical Engineers (ASME) [16]. This matters for base-isolated nuclear facilities in particular. Isolation can substantially reduce superstructure demand, but it concentrates critical performance in the isolation layer and in components crossing the isolation interface, so margin has to be demonstrated there, not only in the superstructure [3,17].

In parallel, modern seismic codes and design workflows still rely heavily on response spectrum (RS) procedures because they reduce a complex time history to period-dependent amplitudes that are easy to use in analysis and design checks [18]. In practice, the target spectrum is often taken from Probabilistic Seismic Hazard Analysis (PSHA) products, most commonly a uniform hazard spectrum (UHS). However, a UHS is not intended to describe a single realizable ground motion, and using it as a matching target can bias record selection. Baker [18] addressed this issue by introducing the conditional mean spectrum (CMS), which links record selection back to PSHA while providing a more realistic expected spectral shape, conditioned on a chosen period. Building on the same idea, Lin, Haselton and Baker [19] proposed the conditional spectrum (CS) with conditional mean and variability to improve hazard consistency in risk-based assessments. Bradley [20] generalized conditional intensity measure (GCIM) framework extends conditioning beyond one measure. It supports consistent selection when more than one intensity measure matters, and it makes the selection choices more explicit. Overall, these tools link record selection to PSHA and keep the procedure practical and transparent.

Critical excitation (CE) methods offer a robust way to deal with the uncertainty of future earthquakes in high-importance systems. The idea goes back to the 1970s. Instead of assuming one representative record, CE defines a physically admissible class of inputs (typically through intensity and other constraints) and then finds the input that produces the largest response in the chosen demand measure [21]. Later work extended the framework to random and nonstationary excitation by placing explicit bounds on the input power spectral density (PSD) (to control power and intensity) and then maximizing the chosen response measure subject to those bounds. [22,23]. A key development for practical studies is the frequency-domain, energy-based form, where the worst-case input is characterized through bounds on earthquake input energy using compact transfer-function expressions [24].

Against this background, this study develops and demonstrates a critical-excitation response-spectrum (CE-RS) framework that remains compatible with code-type spectrum targets while enforcing an explicit energy-consistency constraint. The aim is practical. In early design and in retrofit screening, engineers need fast iterations. Repeating full record selection and scaling after every change is slow. It can also make the iterations inconsistent. Here, the

CE-based spectrum enables a direct, spectrum-level worst-case demand check under rare, BDBE loading assumptions, without rebuilding a record suite each time. The framework also allows a simple resonance check. It shows whether a code-compatible spectrum shape lines up with the main periods of the isolated system. The method is illustrated for base-isolated nuclear structures using global isolation measures, with emphasis on rapid, conservative screening of isolation performance. To our knowledge, this is among the early spectrum-level CE implementations targeted specifically at nuclear isolation checks under code-compatible spectral constraints and an explicit energy bound.

# 2 Modeling of base-isolated NPP structures

This study evaluates CE-based worst-case excitation for a base-isolated nuclear reactor building using a reduced-order dynamic model. The objective is not to reproduce detailed local component response. Instead, the analysis targets the governing horizontal isolation demands, such as peak isolation displacement and the associated base shear, using a model that is clear, numerically stable for parametric studies, and aligned with nuclear isolation guidance and benchmarking work.

Within code-based nuclear seismic workflows, reduced-order models are acceptable when they capture the dominant response characteristics needed to evaluate the global demand measures of interest [15]. Within ASCE/SEI 4-16 workflows [15], simplified structural models are acceptable if they represent the mass–stiffness distribution and resolve the frequency range needed for the response quantities of interest. When significant coupling exists between directional responses, a combined three-dimensional model should be used. Otherwise, separate planar models for individual direction excitations may be used. ASCE/SEI 4-16 also allows lumped-mass (stick-type) models under defined conditions, including cases where the horizontal analysis does not require direct determination of seismic stresses and where torsional effects are appropriately included. ASCE/SEI 43-19 [3] requires that seismic analysis be performed in accordance with ASCE 4 and that modeling follows ASCE 4-16 chapter 3. Therefore, the ASCE 4-16 modeling assumptions adopted here are used to support ASCE 43-19 performance checks focused on global isolation demand.

In this study, the low-damping rubber (LDR) benchmark model proposed by Mir et al. [25] is adopted as a reduced-order representation of the reactor building for isolation-demand screening [25]. Consistent with ASCE/SEI 4-16 simplified modelling options for global response when detailed seismic stresses are not the intended outputs, the model is used to estimate (a) peak horizontal isolation displacement (stroke) and (b) base shear at the isolation plane, and (c) peak absolute acceleration of the lumped superstructure mass as a global response indicator. The focus is the isolation-layer response to horizontal shaking, not detailed superstructure deformation or local component actions. Results from this reduced model are not intended to replace full three-component, coupled evaluations when those are required for final design decisions.

LDR system, shown schematically in Fig. 1, is adopted as a reduced-order representation to evaluate global isolation demand. LDR model is a lightly damped, two-dimensional linear isolation system composed of 17 identical LDR isolators with an effective horizontal isolation period of 2 s. The first horizontal mode in each principal direction occurs at the isolation frequency and carries nearly the full participating mass, indicating that the horizontal response is dominated by the isolation mode and supporting the use of a reduced model when the outputs of interest are peak displacement and global shear demand.

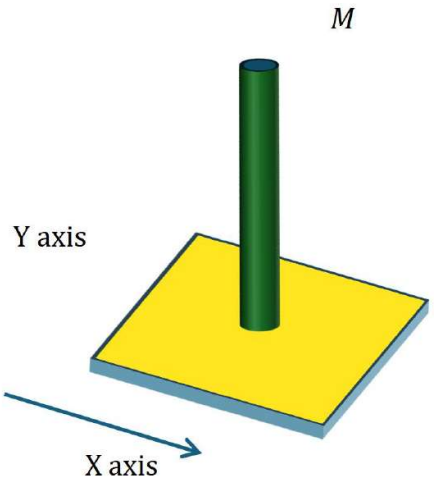


*Figure 1: Representative lumped-mass model for the 2DOF system.*

Mir et al. [25] represent the horizontal dynamics using a two-degree-of-freedom (2DOF) model for performance calculations. The isolated superstructure is treated as rigid above the isolation interface, and the response is governed by one dominant isolation mode in each horizontal direction. The isolation system is represented by an equivalent link element connected between the lumped mass and the ground. The link captures the combined horizontal response of the isolator array (and any damping devices). For LDR model, one equivalent link element (acting in both X and Y) is used. The adopted lumped mass and the effective horizontal stiffness and damping values are summarised in Table 1 [25].

*Table 1: System properties used in the 2DOF model*

| Quantity | Symbol | Value |
|---|---|---|
| Isolated superstructure mass | $M$ | 8,920 ton |
| Horizontal isolation period | $T$ | 2.0 s |
| Equivalent horizontal stiffness | $K$ | 8.8 × 104 kN/m |
| Horizontal viscous damping coefficient | $C$ | 2,800 kN·s/m |

For the present objective, the system idealisation neglects vertical excitation and axial-load fluctuation effects. Previous studies suggest that for isolation systems with high vertical stiffness, variations in axial load during an earthquake usually have a limited effect on peak horizontal isolation displacement. The horizontal input and the isolation properties tend to govern this metric. Vertical shaking may still affect other responses (for example, base shear and floor accelerations), but its influence on peak isolation displacement is often small when reporting global horizontal demands [26]. This supports use of a planar model when the goal is global horizontal isolation demand rather than vertical-sensitive local responses [3, 15, 25].

# 3 Critical Excitation Method (CEM)

In structural dynamics, resonance is the main reason some earthquakes create disproportionate demands. The amplification is not only about how strong the motion is. It happens when the dominant frequency content of the ground motion is close to the natural frequency of the system. Under that condition, even a physically plausible input can drive a large response because energy is transferred efficiently into the critical mode(s) [27].

The CE framework developed by Takewaki extends earlier worst-case formulations and highlights resonance effects more clearly [21]. It searches within an admissible set of ground motions for the one that maximizes a selected response quantity. In practice, the workflow is straightforward. First, describe the system using its dominant modal properties. Next, set a physically reasonable set of input motions using explicit constraints. Then solve the maximization problem to find the worst-case motion.

After the modal properties are identified, the CE problem is written for the adopted structural model [21]. For the 2DOF system used in this study (Section 2), the governing equation is:

$$\mathbf{M}\ddot{\mathbf{u}}(t)+\mathbf{C}\dot{\mathbf{u}}(t)+\mathbf{K}\mathbf{u}(t)=-\mathbf{M}\ddot{\mathbf{u}}_g(t) \tag{1}$$

For the 2DOF system, $\mathbf{M}=\mathrm{diag}(M,M),\mathbf{C}=\mathrm{diag}(C,C)$ , and $\mathbf{K}=\mathrm{diag}(K,K)$ are the diagonal mass, damping, and stiffness matrices, respectively. Moreover, $\mathbf{u}(t)=\lfloor u_X(t)u_Y(t)\rfloor^{\mathrm{T}}$ is the displacement vector. In addition, $\ddot{\mathbf{u}}_g(t)=\left[\ddot{u}_g(t)\quad \ddot{v}_g(t)\right]^{\mathrm{T}}$ denotes the bi-directional orthogonal ground acceleration input. In the following derivation, the CE expressions are written for one horizontal component for clarity; the same form is applied to both $X$ and $Y$.

With the structural model fixed, the CE task is as follows. First, define a realistic admissible set for $\ddot{\mathbf{u}}_g(t)$ . Next, find the input within that set that maximizes the chosen response measure. All constraints must remain satisfied. Because earthquake shaking is nonstationary, the input is written in a envelope representation form [21]:

$$\ddot{u}_g(t)=c(t)w(t) \tag{2}$$

where $c(t)$ is a deterministic envelope and $w(t)$ is a zero-mean stationary process. This separation is practical. The envelope sets how the intensity grows and decays over time, while the stationary part defines the frequency content through its PSD. A standard admissible set in CE is defined by placing constraints directly on the PSD of the stationary component, $S_w(\omega)$. Two core constraints are used. A total power bound and a peak-amplitude bound [21]:

$$\int_{-\infty}^{+\infty} S_w(\omega)\mathrm{d}\omega \le \bar{S}_w \tag{3}$$

$$\sup S_w(\omega) \le \bar{S}_w \tag{4}$$

in which $\bar{S}_w$ is the upper bound on the total spectral area, and $\bar{s}_w$ is the upper bound on the maximum PSD level. It is important to define them here because they set the size of the admissible set from the outset. They are not auxiliary quantities.

Under these constraints, the maximizing PSD becomes rectangular over the active frequency band. This happens because the response is largest when the allowed spectral power is concentrated in the frequency range that most strongly influences the selected response measure. In the same formulation, the band width is written as

$$\Delta\Omega=\bar{S}_w/\bar{s}_w \tag{5}$$

and it is also defined by the lower and upper bounds of the active frequency band:

$$\Delta\Omega = \Omega_U - \Omega_L \tag{6}$$

CE maximizes a chosen response measure. In this study, the objective is the mean-square response $f(t)$ defined later in Eq. (16). The transfer function $H(t,\omega)$ depends only on the fixed structural model $\mathbf{M},\mathbf{C},\mathbf{K}$ and the selected response definition. Under the rectangular-PSD case defined by Eqs. (3)–(6), the objective at each time point $t_i$ reduces to

$$f\left(t_i\right) = \overline{s}_w \int_{\Omega_L}^{\Omega_U} H\left(t_i,\omega\right) \mathrm{d}\omega \tag{7}$$

The CE result is obtained by evaluating $f\left(t_i\right)$ over the considered time window and choosing the time $t_i$ that maximizes it. In Eq. (7), $H\left(t_i,\omega\right)$ is the system transfer function for the selected response measure. It is determined by the structural model $\mathbf{M},\mathbf{C},\mathbf{K}$, damping, and the chosen response definition, and it describes how input spectral content at frequency $\omega$ contributes to the response level at time $t_i$. Therefore, maximizing $f\left(t_i\right)$ corresponds to placing the admissible spectral power inside the frequency band where $H\left(t_i,\omega\right)$ is most influential, while satisfying the PSD bounds in Eqs. (3)–(4) and the additional intensity constraints in Eqs. (8)–(13) [21].

PSD bounds alone may allow unrealistic inputs if they are not constrained by physical intensity measures. For that reason, additional constraints are imposed using Arias intensity and peak measures namely peak ground acceleration (PGA) and peak ground velocity (PGV). A key link is provided by Parseval-type relations in the frequency and time domains:

$$\int |A(\omega)|^2 \, \mathrm{d}\omega = 2\pi \int \ddot{u}_g^2(t) \mathrm{d}t = 4gI_A \tag{8}$$

and the Arias intensity is defined as

$$I_A = \frac{\pi}{2g} \int \ddot{u}_g^2(t) \mathrm{d}t \tag{9}$$

Then the admissible set is tightened using bounds such as

$$I_A \le \overline{I}_A \tag{10}$$

$$\sup |\, A(\omega)| \le \overline{A} \tag{11}$$

where $A(\omega)$ is the acceleration spectrum and $\overline{A}$ is the corresponding upper bound on its magnitude. Under these bounds, and for a rectangular spectrum, the admissible active bandwidth $\Delta\Omega$ follows as

$$\Delta\Omega = \frac{4\pi \overline{I}_A}{\overline{A}^2} \tag{12}$$

To control long-period content consistently with PGV-type limits, the acceleration and velocity spectra are connected through

$$A(\omega) = \mathrm{i}\,\omega V(\omega) \tag{13}$$

where $V(\omega)$ is the velocity spectrum and $\mathrm{i} = \sqrt{-1}$ is the imaginary unit. In this way, bounds on velocity-based measures also limit low-frequency energy. Without these bounds, low-frequency content could become too large and lead to overly conservative displacement demands. Fig. 2 illustrates how the acceleration- and velocity-related constraints act together in practice.

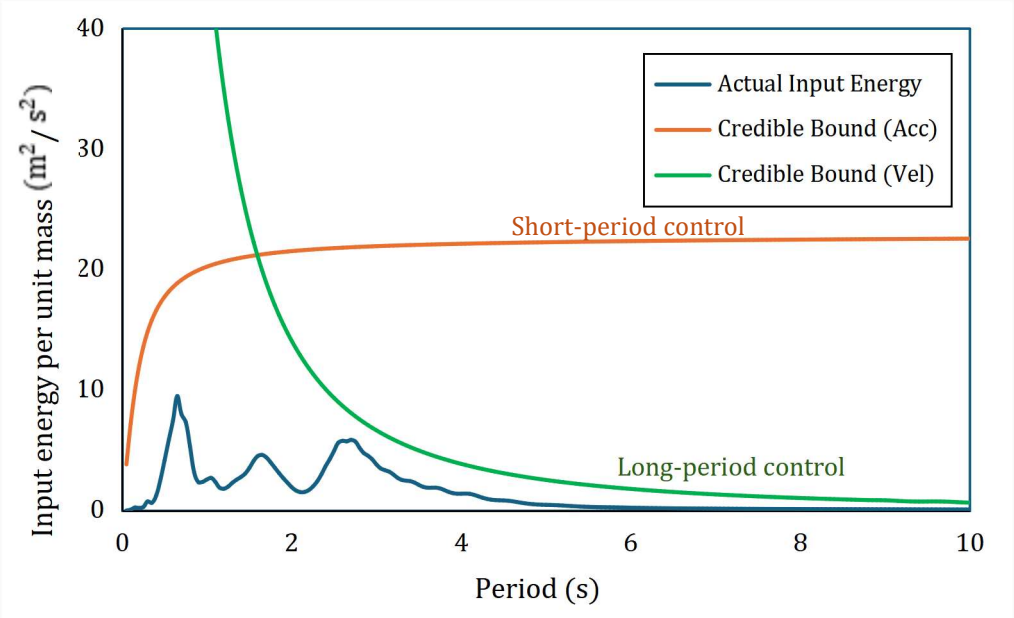


*Figure 2: Period-dependent input energy and credible bounds for CE constraints (acceleration and velocity controls).*

The single rectangular PSD proposed by Takewaki is intentionally sharp. It pushes the allowable power directly into the most damaging band. That is good for identifying a worst case, but it can be too concentrated compared with real records. To improve realism while keeping the same admissible logic, Bazrafshan et al. [28] proposed a three-segment PSD that spreads energy more naturally across a broader band but at lower levels away from the dominant peak. A convenient three-segment form is:

$$S_\omega = \begin{cases} 0; & \omega < \omega_l \\ S_1; & \omega_l < \omega < a \\ S_2; & a < \omega < b \\ S_1; & b < \omega < \omega_h \\ 0; & \omega_h < \omega \end{cases} \tag{14}$$

with

$$S_1 = \frac{\bar{S}_w - \Delta\Omega \bar{S}_w}{(\omega_h - \omega_l) - \Delta\Omega} \tag{15}$$

In this setup, the middle segment targets the critical band (around the dominant system period), while the side segments preserve the total spectral area and avoid an unrealistically narrow spike. Fig. 3 shows the geometry of the three segments and the meaning of $\omega_l, \omega_h, a, b$ .

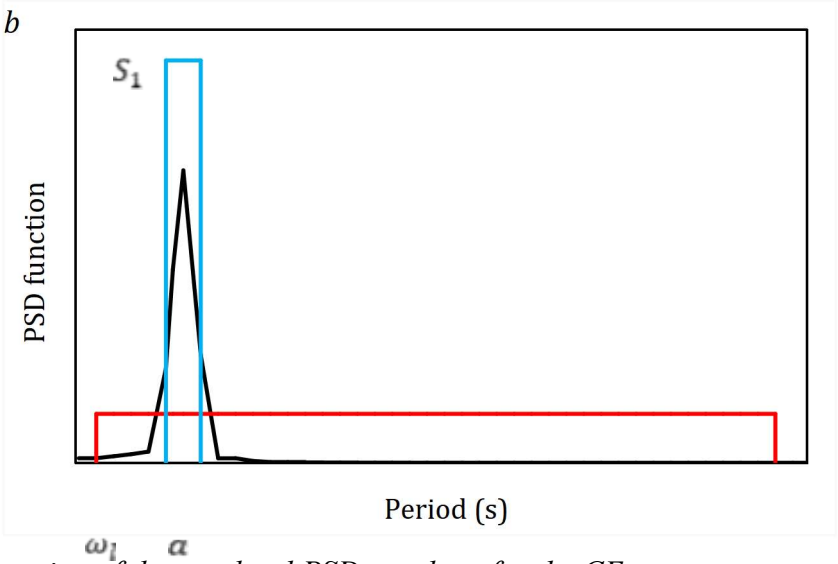


*Figure 3: Illustration of the two-level PSD envelope for the CE.*

A CE analysis is most meaningful when the maximized response quantity matches the decision objective. In the CE literature, interstory drift is a common objective because it links directly to damage and performance limits, and it is the objective adopted in our earlier CE procedure [21]. For nuclear-oriented screening, our recent work further adapted CE for nuclear practice and again showed that a displacement-based objective is a rational choice when the goal is to bound displacement-sensitive demands and avoid non-conservative acceleration-only screening [29]. For resonance-focused problems in long-period or base-isolated systems, displacement remains the governing demand because it controls isolator stroke, deformation compatibility, and impact/pounding potential.

The objective can be written in a mean-square form using the transfer function:

$$f(t) = \sum_{k=1}^{n} x_k^2(t) = \int_{-\infty}^{+\infty} H(t,\omega) S_w(\omega) \mathrm{d}\omega \tag{16}$$

In a linear system, the transfer-function $H(t,\omega)$ follows from the modal (or impulse-response) representation of the system. It depends on the system and the selected response quantity, not on the particular choice of $S_w(\omega)$ . This relation links the system behavior to the worst-case input search. In CE, the admissible PSD is defined by Eqs. (3)–(4) (and, if used, Eqs. (14)–(15)). The procedure allocates this PSD to the frequency region that maximizes the integral in Eq. (16), while satisfying the physical constraints in Eqs. (8)–(13) [21].

# 4 Ground motion selection

Record selection has a major impact on nonlinear time-history results. This is especially true for base-isolated nuclear systems, where the response is dominated by a narrow frequency band near the isolation period. We use the Diablo Canyon Power Plant site in California as the case-study site. The site has extensive published seismic-hazard work, including long-term

program studies and later confirmatory assessments. It has also been used as a benchmark site in studies of seismically isolated nuclear structures under hazard-consistent motions. This makes the hazard target and the record-selection basis more transparent and easier to justify [30, 31].

Diablo Canyon Power Plant sits on the central California coast within the active Pacific–North America plate-boundary zone. The site hazard is strongly influenced by nearby offshore right-lateral faults, most notably the Hosgri and Shoreline fault systems. For broader context, the 2023 update of the U.S. National Seismic Hazard Model incorporates revised rupture forecasts and ground-motion components and provides updated UHS across the western U.S. [30].

To keep record selection transparent and reproducible, we start from the recorded-motion set developed for the Diablo Canyon Power Plant site in Ref. [31]. That study assembled 30 recorded ground motions from the Pacific Earthquake Engineering Research Center; Next Generation Attenuation—West2 (PEER NGA-West2) database, which provides consistently processed strong-motion time series and metadata for shallow crustal earthquakes in active tectonic regions [32]. The motions were then spectrally matched to the site's 10,000-year uniform-hazard response spectrum (UHRS) for a reference rock condition (Site Class B). This approach keeps the suite hazard-consistent while retaining real recorded waveforms as the starting point [31].

From the 30-record pool, we select an 11-record subset (Table 2). The subset is chosen to (i) remain compatible with the Diablo Canyon UHRS target and its key hazard contributors, and (ii) reduce computational cost for repeated nonlinear analyses. The screening uses the following criteria:

- **Hazard consistency.** Retain motions whose matched spectra remain consistent with the UHRS basis and the analysis spectrum level used in the workflow [3, 15].
- **Event realism.** Prefer records whose magnitude, distance, and mechanism are broadly consistent with the main PSHA disaggregation contributors at the target hazard level [30].
- **Directivity pulses.** Avoid suites dominated by strong pulse-like motions when pulses are not representative of the dominant hazard contributors at the site. Pulse identification follows established methods [33].
- **Outlier control.** Remove records with atypical intensity characteristics that would shift the suite mean and dispersion away from the intended hazard-consistent target.

*Table 2: Ground motion records used in this study*

| Events | RSN | Mw |
|---|---|---|
| San Fernando | 72 | 6.61 |
| San Fernando | 77 | 6.61 |
| Loma Prieta | 810 | 6.93 |
| Loma Prieta | 763 | 6.93 |
| Northridge | 1021 | 6.69 |
| Northridge | 1051 | 6.69 |
| Chi-Chi | 2704 | 6.2 |
| Irpinia | 284 | 6.9 |
| Manjil | 1633 | 6.4 |
| Cape Mendocino | 828 | 7.0 |
| Kocaeli | 1161 | 7.5 |

# 5 Numerical analyses

## 5.1 General remarks

Section 2 introduced the reduced-order model, which is used here for the numerical analyses [25]. The focus is global isolation-layer response. The reported outputs are (a) peak horizontal isolation displacement (stroke), (b) base shear at the isolation plane, and (c) peak absolute acceleration of the lumped superstructure mass as a global indicator. This focus keeps the comparison clear. It links changes in the input spectrum to changes in the key isolation response. Local superstructure responses are not included because they are outside the scope of this study.

The case-study site is Diablo Canyon, California. The design-level target spectrum is the ASCE 43 design response spectrum (DRS). In the ASCE 43 workflow, the DRS is obtained by scaling the UHRS for the target performance goal (TPG) associated with the selected seismic design category (SDC) [3]. In this study, SDC 5 is used because it corresponds to the highest seismic design category, where the consequences of unacceptable performance are greatest. In ASCE 43 terminology, it corresponds to a TPG of $1\times10^{-5}$ mean annual frequency of seismic damage exceeding the assigned limit state [3]. Accordingly, we adopt DRS-5 (the SDC-5 DRS) for Diablo Canyon as the baseline design-level spectrum. Figure 4 shows the DRS-5 shape and the scale factors for the selected site/soil definition. These follow the ASCE 43 DRS construction procedure [34].

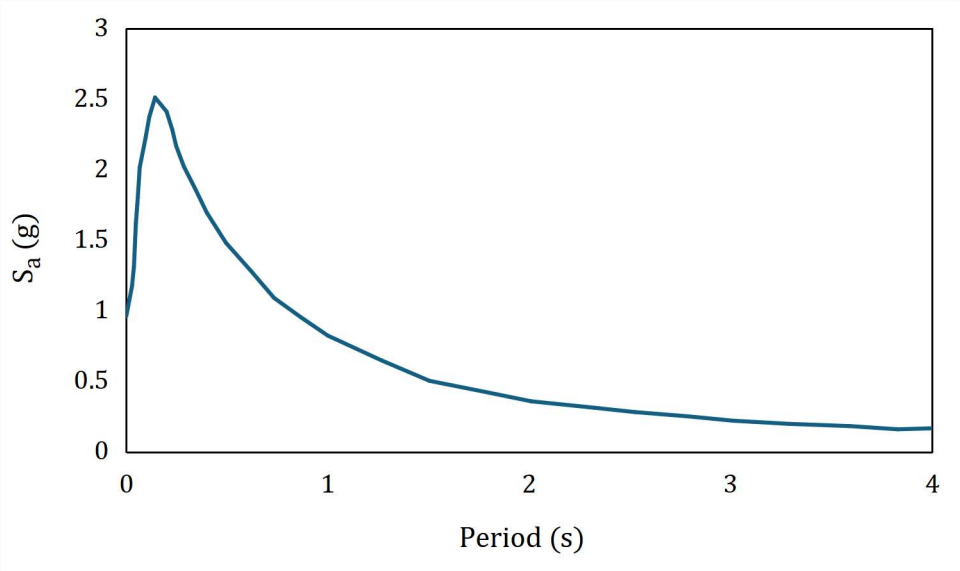


*Figure 4: Diablo Canyon design response spectrum for SDC 5 (DRS-5).*

After the 2011 Tohoku/Fukushima accident, nuclear seismic practice put more emphasis on explicitly checking hazards and demands beyond the original design basis. IAEA guidance formalizes the need to consider higher-than-design conditions through design-extension or BDBE concepts in design and assessment, including external hazards such as earthquakes [1,2].

In this study, we keep the ASCE 43 design-level spectrum [3] as the baseline and build BDBE cases by controlled scaling. ASCE/SEI 43-19 defines the design RS as DRS = SF × UHRS at the target performance goal, and it states that SDC 5 corresponds to $P = 1 \times 10^{-5}$ mean annual frequency of unacceptable performance. Accordingly, we use DRS-5 for Diablo

Canyon as the base shape and define BDBE spectra as 150%, 167%, and 200% of DRS. This approach is common in nuclear studies as a practical way to represent stronger than design shaking for robustness checks[35]. These scaled cases are not a substitute for re-deriving a new UHRS at a different exceedance level. They are used here to keep the hazard-based DRS shape fixed and to make the demand trends with increasing intensity easy to interpret and compare. Figure 5 shows DRS-5 for Diablo Canyon, the BDBE scaling cases, and the CE-RS used in the analyses.

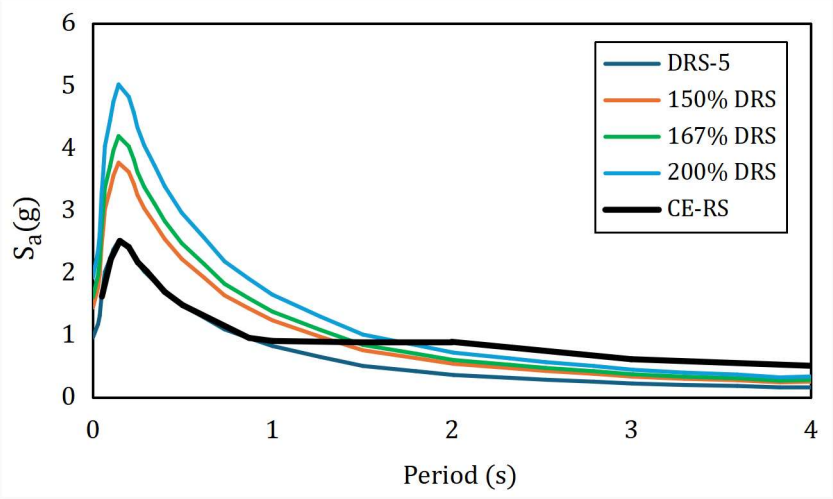


*Figure 5: Diablo Canyon target spectra used in this study: ASCE 43 design response spectrum for SDC 5 (DRS-5), the BDBE-scaled spectra (multipliers of DRS-5), and the CE-based response spectrum (CE-RS).*

To compare the CE procedure against the DRS and the BDBE-scaled spectra, the CE admissible set must be anchored to physical intensity measures. We therefore use at least one recorded earthquake motion as a baseline. From the selected horizontal component(s), we compute PGA, PGV, and Arias intensity. These values are then used as bounds to define the CE constraints, and the same constraint set is applied consistently across the parametric cases.

Because the case-study site is Diablo Canyon in California, we adopt the 1989 Loma Prieta earthquake as a historically important California strong-shaking event documented by United States Geological Survey (USGS) products. USGS reports describe the event and summarize the strong-motion dataset and its regional shaking characteristics. The record-derived intensity measures are computed from the chosen component(s) and then used to set the CE constraints for all comparisons.

For response-history evaluation under spectrum-compatible motions, we use 11 sets of horizontal ground motions. This gives stable mean demand estimates and reduces sensitivity to record-to-record variability in the global isolation metrics. This choice follows common nonlinear time-history practice and is also consistent with recent nuclear isolation guidance that discusses the use of at least 11 record sets [31].

Each record is scaled (spectrally matched) to the target spectrum so that all comparisons are anchored to the same baseline definition (DRS-5) and its BDBE multipliers, as well as the CE-RS. The reported demand measures are (i) maximum resultant horizontal isolation displacement, (ii) base shear at the isolation plane, and (iii) peak absolute acceleration of the lumped superstructure mass as a global indicator.

As an internal check, we also compare CE results obtained from the Loma Prieta–based constraints with CE results obtained when the constraints are derived from a representative spectrum-compatible (scaled/matched) record. This comparison helps verify that the CE

trends are not driven by a single baseline record and supports the validation of the CE procedure against the DRS/BDBE/CE-RS response-history results.

Fig. 6 summarizes the mean results from the 11-record set for peak isolation displacement, base shear, and peak absolute acceleration. As expected, the BDBE scaling cases produce larger demands than DRS-5. This follows the increase in spectrum amplitude shown in Fig. 5. The CE-RS case gives the largest demands across all three metrics, and the trend is consistent with the fact that the CE-RS target is higher than the BDBE-scaled spectra over the periods that control the isolation response. This pattern suggests that DRS-5 and the BDBE-scaled spectra may still underestimate resonance-driven demands for this isolated system. They reflect hazard-level scaling, but they do not explicitly target the frequency band that maximizes the isolation response under resonance.

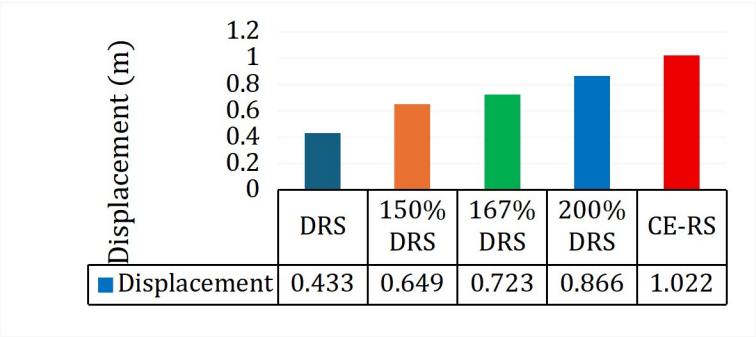


(a)

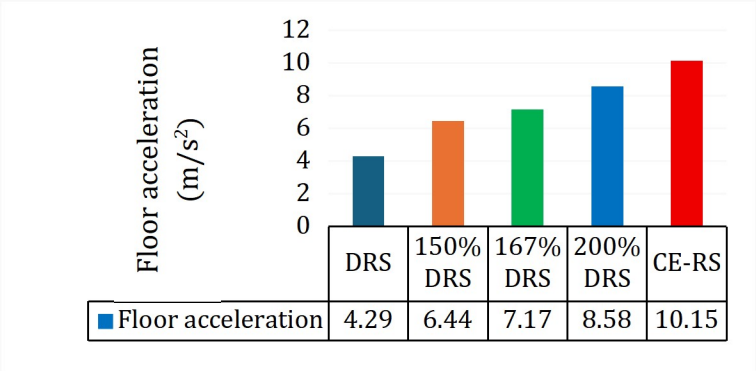


(b)

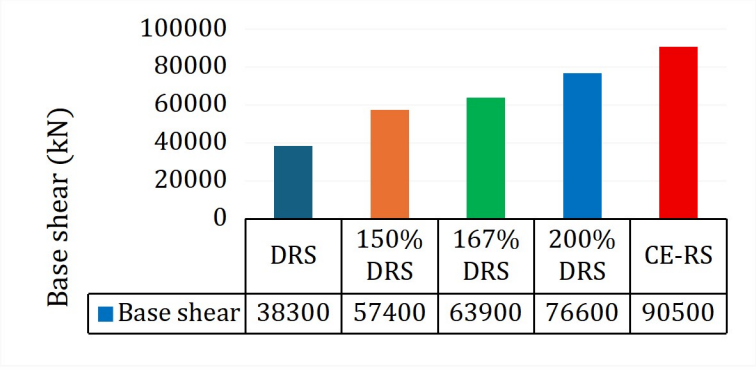


(c)

*Figure 6: Mean global isolation responses from the 11-record spectrum-compatible analyses for Diablo Canyon: (a) peak resultant isolation displacement, (b) peak absolute acceleration at the lumped superstructure mass, and (c) base shear.*

The key point is how the CE-RS is obtained. The CE-RS is not defined by simply increasing the hazard level. Instead, it is derived by maximizing the selected response measure within an admissible set that satisfies the same physical and intensity constraints. In other words, it uses the available input energy in a way that is most damaging to the system. This highlights a resonance-driven effect. Demands increase when the input frequency content aligns with the dominant period(s) of the isolated system. Therefore, a DRS or a scaled BDBE spectrum may still miss response-controlling spectral features, even when the overall intensity level is increased, if the frequency content does not concentrate around the most influential band for the isolation mode.

To check the validity of the CE results, Table 3 reports the CE-based responses when the admissible set constraints are derived from the selected Loma Prieta record component(s). The resulting demands are in very close agreement with the CE-RS results in Fig. 6, with differences below about 1%. This consistency indicates that the CE outcome is not sensitive to the specific baseline record used to define the intensity constraints, and it supports the robustness of the CE procedure for the present screening study.

*Table 3: CE-based mean global isolation responses obtained using Loma Prieta–derived intensity constraints*

| Response metrics | CE Loma Prieta |
|---|---|
| Displacement (m) | 1.032 |
| Floor acceleration (m/s$^2$) | 10.24 |
| Base shear (kN) | 91300 |

Overall, the spectrum-based CE workflow provides a fast and traceable supplement to code-based spectra. It is not intended to replace ASCE/NRC/IAEA design and verification procedures. Instead, it provides an additional early-stage check to identify whether resonance-sensitive isolation demands may be underestimated by standard DRS/BDBE scaling. The same idea can also be useful for existing isolated systems, where it can support strengthening or rehabilitation planning by quickly screening demand increases under resonance-driven input shaping.

# 6 Conclusions

This study evaluated global isolation-layer demands for a base-isolated nuclear reactor building using a reduced-order 2DOF model. The focus was on three global metrics, peak horizontal isolation displacement, base shear, and peak absolute acceleration at the lumped superstructure mass. Using the Diablo Canyon site as the case study, DRS-5 (SDC 5) was adopted as the baseline design spectrum, and beyond-design-basis levels were represented by controlled multipliers of the same DRS shape (150%, 167%, and 200%). Nonlinear response-history analyses were performed with 11 spectrum-compatible ground-motion sets to obtain stable mean estimates of the global demands.

Across all metrics, demand increased with BDBE scaling, as expected from the increase in spectrum amplitude. However, the CE-RS produced the largest demands, even relative to the higher BDBE multipliers. This indicates that standard DRS/BDBE scaling may not fully capture resonance-driven isolation demands for long-period or base-isolated systems. The key

difference is not only intensity. CE-RS is obtained by maximizing the selected response measure within an admissible input set that satisfies the same physical and intensity constraints. It therefore concentrates admissible frequency content in the band that most strongly excites the isolation mode and can increase displacement-sensitive demands when resonance conditions occur.

A validation check was also performed by defining CE constraints from a historically relevant recorded event (the 1989 Loma Prieta earthquake). The CE responses based on Loma Prieta-derived constraints were consistent with the CE-RS-based results, with differences below about 1%. This supports the robustness of the CE procedure for the present screening objective and suggests that the results are not driven by a single baseline record choice.

The spectrum-based CE workflow is a fast and traceable supplement to code-based spectra. It is suitable for early-stage design because it can quickly flag resonance-sensitive isolation demands that may not be evident from DRS/BDBE scaling alone. It is also useful for existing isolated facilities, where it can support strengthening or rehabilitation planning by screening how isolation displacement, base shear, and global acceleration indicators change under resonance-driven input shaping. The method is not intended to replace ASCE/NRC/IAEA design and verification procedures. Future work should test the CE-RS screening with higher-fidelity 3D models (including torsion/coupling, nonlinear isolators, and vertical effects where relevant) and across multiple sites/hazard conditions. It should also extend the outputs beyond global isolation demand to include nuclear-relevant measures such as in-structure spectra and key component demands, to define where CE screening adds the most value in code-familiar workflows.

# Acknowledgments

The first author would like to express his appreciation for the scholarship provided by the Ueda Foundation during his Ph.D. studies at Hiroshima University.

# References

[1] International Atomic Energy Agency (IAEA) (2021) *Seismic Design for Nuclear Installations.* IAEA Safety Standards Series No. SSG-67. Vienna: IAEA.

[2] International Atomic Energy Agency (IAEA) (2024) *Evaluation of Seismic Safety for Nuclear Installations.* IAEA Safety Standards Series No. SSG-89. Vienna: IAEA.

[3] American Society of Civil Engineers (ASCE) (2020) *Seismic Design Criteria for Structures, Systems, and Components in Nuclear Facilities.* ASCE/SEI 43-19. Reston, VA: ASCE. ISBN 9780784482407.

[4] Douglas, J., Crowley, H., Silva, V., Marzocchi, W., Danciu, L. and Pinho, R. (2024) 'Methods for evaluating the significance and importance of differences amongst probabilistic seismic hazard results for engineering and risk analyses: A review and insights', *Bulletin of Earthquake Engineering*, 22(6), pp. 2769–2796. https://doi.org/10.1007/s10518-024-01896-y

[5] Uang, C.-M. and Bruneau, M. (2018) 'State-of-the-art review on seismic design of steel structures', *Journal of Structural Engineering (ASCE)*, 144(4), 03118002. https://doi.org/10.1061/(ASCE)ST.1943-541X.0001973

[6] Unjoh, S., Terayama, T., Adachi, Y. and Hoshikuma, J.-i. (2000) 'Seismic retrofit of existing highway bridges in Japan', *Cement and Concrete Composites*, 22(1), pp. 1–16. https://doi.org/10.1016/S0958-9465(99)00043-8

[7] Bray, J.D. and Rodríguez-Marek, A. (2004) 'Characterization of forward-directivity ground motions in the near-fault region', *Soil Dynamics and Earthquake Engineering*, 24(11), pp. 815–828. https://doi.org/10.1016/j.soildyn.2004.05.001

[8] Elnashai, A.S., Gencturk, B., Kwon, O.-S., Hashash, Y.M.A., Kim, S.J., Jeong, S.-H. and Dukes, J. (2012) 'The Maule (Chile) earthquake of February 27, 2010: Development of hazard, site specific ground motions and back-analysis of structures', *Soil Dynamics and Earthquake Engineering*, 42, pp. 229–245. https://doi.org/10.1016/j.soildyn.2012.06.010

[9] Marshall, J., Jaiswal, K.S., Gould, N., Turner, F., Lizundia, B. and Barnes, J. (2013) 'Post-earthquake building safety inspection: Lessons from the Canterbury, New Zealand, earthquakes', *Earthquake Spectra*, 29(3), pp. 1091–1107. https://doi.org/10.1193/1.4000151

[10] Chandramohan, R., Baker, J.W. and Deierlein, G.G. (2016) 'Impact of hazard-consistent ground motion duration in structural collapse risk assessment', *Earthquake Engineering and Structural Dynamics*, 45(8), pp. 1357–1379. https://doi.org/10.1002/eqe.2711

[11] Harati, M. and van de Lindt, J.W. (2024) 'Mainshock-aftershock building fragility methodology for community resilience modeling', *Structures*, 70, 107742. https://doi.org/10.1016/j.istruc.2024.107742

[12] Takewaki, I., Murakami, S., Fujita, K., Yoshitomi, S. and Tsuji, M. (2011) 'The 2011 off the Pacific coast of Tohoku earthquake and response of high-rise buildings under long-period ground motions', *Soil Dynamics and Earthquake Engineering*, 31(11), pp. 1511–1528. https://doi.org/10.1016/j.soildyn.2011.06.001

[13] Takewaki, I., Fujita, K. and Yoshitomi, S. (2013) 'Uncertainties in long-period ground motion and its impact on building structural design: Case study of the 2011 Tohoku (Japan) earthquake', *Engineering Structures*, 49, pp. 119–134. https://doi.org/10.1016/j.engstruct.2012.10.038

[14] Konno, K. and Toyoda, M. (2023) 'Change in dynamic characteristics of base-isolated buildings with irregular shape based on long-term vibration records', *Journal of Japan Association for Earthquake Engineering*, 23(6).

[15] American Society of Civil Engineers (ASCE) (2017) *Seismic Analysis of Safety-Related Nuclear Structures.* ASCE/SEI 4-16. Reston, VA: ASCE.

[16] American Society of Mechanical Engineers and American Nuclear Society (ASME/ANS) (2021) *Probabilistic Risk Assessment Standard for Advanced Non-Light Water Reactor Nuclear Power Plants.* ANSI/ASME/ANS RA-S-1.4-2021. New York, NY: ASME/ANS.

[17] Kumar, M., Whittaker, A.S. and Constantinou, M.C. (2015) *Seismic Isolation of Nuclear Power Plants Using Elastomeric Bearings.* MCEER-15-0008. Buffalo, NY: MCEER, University at Buffalo.

[18] Baker, J.W. (2011) 'The conditional mean spectrum: A tool for ground motion selection', *Journal of Structural Engineering (ASCE)*, 137(3), pp. 322–331. https://doi.org/10.1061/ (ASCE)ST.1943-541X.0000215

[19] Lin, T., Haselton, C.B. and Baker, J.W. (2013) 'Conditional spectrum-based ground motion selection. Part I: Hazard consistency for risk-based assessments', *Earthquake Engineering and Structural Dynamics*, 42(12), pp. 1847–1865. https://doi.org/10.1002/eqe.2301

[20] Bradley, B.A. (2010) 'A generalized conditional intensity measure approach and holistic ground motion selection', *Earthquake Engineering and Structural Dynamics*, 39(12), pp. 1321–1342. https://doi.org/10.1002/eqe.995

[21] Takewaki, I. (2013) *Critical Excitation Methods in Earthquake Engineering.* 2nd edn. Oxford: Butterworth-Heinemann.

[22] Takewaki, I. (2002) 'Seismic critical excitation method for robust design: A review', *Journal of Structural Engineering (ASCE)*, 128(5), pp. 665–672. https://doi.org/10.1061/ (ASCE)0733-9445(2002)128:5(665)

[23] Takewaki, I. (2001) 'Nonstationary random critical excitation for acceleration response', *Journal of Engineering Mechanics (ASCE)*, 127(6), pp. 544–556. https://doi.org/10.1061/ (ASCE)0733-9399(2001)127:6(544)

[24] Takewaki, I. (2004) 'Bound of earthquake input energy', *Journal of Structural Engineering (ASCE)*, 130, pp. 1289–1297. https://doi.org/10.1061/(ASCE)0733-9445(2004)130:9(1289)

[25] Mir, F.U.H., Yu, C.-C., Carmichael, B.M., Chisholm, B.M., Redd, J., Talaat, M.M., Bolisetti, C. and Whittaker, A.S. (2025) *Guidelines for Implementing Seismic Base Isolation in Advanced Nuclear Reactors (Technical Report MCEER-24-0001, Rev. 01).* Buffalo, NY: MCEER, University at Buffalo.

[26] Mosqueda, G., Whittaker, A.S. and Fenves, G.L. (2004) 'Characterization and modeling of friction pendulum bearings subjected to multiple components of excitation', *Journal of Structural Engineering (ASCE)*, 130(3), pp. 433–442. https://doi.org/10.1061/(ASCE)0733-9445(2004)130:3(433)

[27] Chopra, A.K. (2017) *Dynamics of Structures: Theory and Applications to Earthquake Engineering.* 5th edn. Hoboken, NJ: Pearson. ISBN 9780134555126.

[28] Bazrafshan, A., Khaji, N. and Ahmadi, G. (2024) 'A new probabilistic long-period critical excitation procedure for isolated building structures', *Mechanics Based Design of Structures and Machines*, 52(9), pp. 7063–7091. https://doi.org/10.1080/15397734.2023.2297242

[29] Ahmadi, A., Khaji, N. and Sadegh-Azarb, H. (2026) 'Beyond-design-basis screening by a three-bound critical excitation envelope for base-isolated nuclear power plants', *Nuclear Engineering and Design*. https://doi.org/10.1016/j.nucengdes.2025.114700

[30] Petersen, M.D. et al. (2024) 'The 2023 US 50-State National Seismic Hazard Model: Overview and implications', *Earthquake Spectra*, 40(1), pp. 5–88. https://doi.org/10.1177/87552930231215428

[31] Kumar, M., Whittaker, A.S. and Constantinou, M.C. (2015) *Seismic Isolation of Nuclear Power Plants Using Sliding Bearings.* MCEER-15-0006. Buffalo, NY: MCEER, University at Buffalo.

[32] Bozorgnia, Y., Abrahamson, N.A., Al Atik, L., Ancheta, T.D., Atkinson, G.M., Baker, J.W., Baltay, A.S., Boore, D.M., Campbell, K.W., Chiou, B.S.J., Darragh, R.B., Day, S., Donahue, J., Graves, R.W., Gregor, N., Hanks, T., Idriss, I.M., Kamai, R., Kishida, T., Kottke, A., Mahin, S.A., Rezaeian, S., Rowshandel, B., Seyhan, E., Shahi, S., Shantz, T., Silva, W., Spudich, P., Stewart, J.P., Watson-Lamprey, J., Wooddell, K. and Youngs, R. (2014) 'NGA-West2 research project', *Earthquake Spectra*, 30(3), pp. 973–987. https://doi.org/10.1193/072113EQS209M

[33] Shahi, S.K. and Baker, J.W. (2014) 'An efficient algorithm to identify strong-velocity pulses in multicomponent ground motions', *Bulletin of the Seismological Society of America*, 104(5), pp. 2456–2466. https://doi.org/10.1785/0120130191

[34] Yu, C.-C. and Whittaker, A.S. (2024) 'Generating seismic design basis spectra for US nuclear energy facilities', *Nuclear Engineering and Design*, 426, 113333. https://doi.org/10.1016/j.nucengdes.2024.113333

[35] Kumar, M., Whittaker, A.S. and Constantinou, M.C. (2015) 'Response of base-isolated nuclear structures to extreme earthquake shaking', *Nuclear Engineering and Design*, 295, pp. 860–874. https://doi.org/10.1016/j.nucengdes.2015.06.005